The role of acquisition geometry and components for imaging microseismicity

*Zhihui Zou** [1, 2], *Huawei Zhou*[1, 2], *Fan Jiang*[1], *and Hui Liu*[1],
[1] *Departments of Geosciences, Texas Tech University*
[2] *Tomographysic Earth System Imaging Center, China University of Geosciences*

Summary

Radiation pattern of microseismicity is an important indicator of fracture orientation and distribution during reservoir fluid injection events. The quality of mapping the source radiation pattern by reverse time modeling is evaluated here. Among many factors influencing the imaging quality, the acquisition geometry and the component of input data are the most important. For instance, using a straight line of receivers will resulted in two imaged sources: the true source and a mirror source. The amplitudes of the two imaged sources are the same for single-component data, but the true imaged source has much higher amplitude than that of the mirror source for two-component data. One way to improve the image quality is to increase the array aperture, such as using both surface and wellbore receivers rather than just the surface receivers. Our results show that a larger aperture will result in better imaged source that matches well with the true source in both amplitude distribution and angle distribution of displacement. Those results will be useful for reservoir monitoring acquisition design and the study of induced microseismicity.

Introduction

Mapping induced seismicity due to fluid injection in reservoirs is significant for understanding the stress field and fracture distribution that may dictate fluid migration. Such a source imaging problem consists of two parts: determining the source location and imaging the source radiation pattern. While many methods exist for imaging sources, we focus on the reverse time modeling (RTM) method in this study.

The RTM can be carried out using acoustic or elastic waves. Using acoustic waves is popular for migration (Loewenthal and Mufti, 1983; Baysal *et al*., 1983) and source location (Gajewski and Tessmer, 2005; Lu and Toksöz, 2008), because it has low cost and less artifacts than elastic reverse time method (Chang and McMechan, 1987; Sun and McMechan, 2001). Elastic RTM has been used to map the source mechanism (Hu and McMechan, 1988), but there has not been a quantitative analysis on the resolution of mapping the source. Recent years have seen the use of RTM to locate the microseismicity caused by fluid injection (Gajewski and Tessmer, 2005; Lu and Toksöz, 2008). This study focus on assessing the efficiency of elastic RTM in mapping microseismicity.

There are two main factors influencing the source imaging. The first factor is the components of the input data. If we use a straight line of receivers, the RTM will map out an imaged source at the true source position plus a mirror source, and the two imaged sources are located symmetric with respect to the receiver line. The availability of data components significantly influences the amplitude ratio of the mirror source versus that of the true source. The amplitude of the mirror source will be much less than that of the true source if we use two-component data in 2D case, in contrast to the same amplitude if we use one-component data. The second factor is the acquisition geometry. The acquisition geometry may be quantified in term of the aperture (Hu and McMechan, 1988). Two kinds of acquisition geometries are compared in this paper: receivers on surface and receivers on both surface and in wellbores. The aperture of the first geometry is less than that of the second. We evaluate the quality of an imaged source based on its distributions in amplitude and displacement orientation. The results of RTM show that the larger the aperture, the better quality of the source imaged.

Assessment on the Resolution of Source imaging

To assess the resolution of the imaged source, we created some synthetic models and the testing data using forward modeling, and then conducted reverse time modeling. The purpose of the forward modeling is to calculate the synthetic seismograms as the input data. Here a pseudo-spectral elastic forward modeling (Kosloff *et al*, 1984) is used to calculate elastic wave field. To simulate the double-couple source mechanism which occurs most commonly for natural earthquakes, we used a combination of four point forces (White, 1965).

Reverse time modeling is to solve a boundary condition problem of wave equation (Chang and McMechan, 1987). We use the same numerical method in forward modeling to calculate the wave field. The recorded seismograms are viewed as the boundary values of a wave equation. During RTM processing the recorded seismic waves are reversed in time and input into the receivers as source functions. Each receiver can be considered as an individual source, and the whole reverse time wave field is the combination of the wave fields from all receivers. The imaging time is determined by the time shift of the largest amplitude of wavelet used in the forward modeling.

The role of input components in source imaging

For the case that the seismic waves are recorded by one receiver array along a straight line, we know there will be a mirror source on the other side of the receiver line. This also occurs when the receivers lie along a well. In reality the seismic waves may be recorded by one component or three components sensors. Our results show that the amplitude of the RTM image is much higher at the true source position than that of at the mirror source position for multi-component data. But the amplitude is the same at the true source and mirror source positions if the input data is single component.

To show the influence of the data components on imaged source a 2D synthetic test was created and the results are shown in Figure 1. Receivers, represented by the triangles in Figure 1, are set along a well at the center of the depth slice to record a double-couple source. Figure 1a shows the true source location and amplitude distribution. The imaged wave fields are illustrated in Figure 1b, 1c, and 1d which represent elastic RT modeling using two-component data, the vertical and horizontal component data respectively. The black curves in those figures are the relative amplitude at 710 m in depth, the depth of the source. The color scale in each figure shows the energy distribution of the wave field.

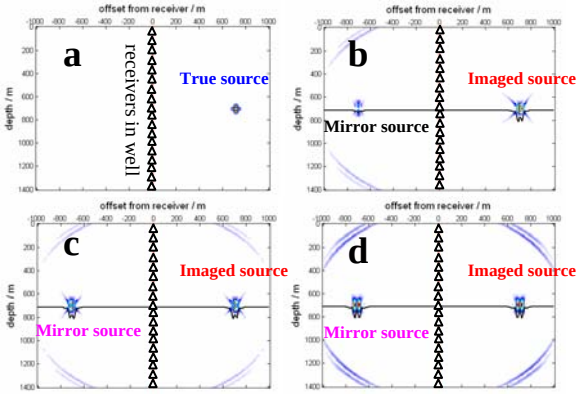

Figure 1: Depth slice illustrating the wave field amplitude distribution. a. Locations of true source and receivers; b, c, and d are wave field energy distribution. b: using two–component data; c: using vertical component data; d: using horizontal component data.

There are two large energy peaks in Figures 1b, 1c, and 1d. The energy peak on the right side of the receiver array is the imaged source, and the peak on the left side of receivers is the mirror source. We draw a line through the source to show the relative amplitude of the imaged source and the mirror source. If the data is two components the peak energy of the imaged source is much higher than that of the mirror source; the ratio between them is about 3.4 as shown in Figure 1b. If the input data is just one component, either the vertical component in Figure 1c or horizontal component in Figure 1d, the peak energy of the imaged source is equal to that of the mirror source.

In real reservoir monitoring the influence of the mirror source will be significant when there are only a few of wells and the receivers are located closed to each other. In that case elastic records are necessary to distinguish the mirror source from the true source locations.

The role of acquisition geometries in source imaging

In reality the seismic waves are recorded by receivers that are distributed at certain locations, and this is the acquisition geometry. Two of the acquisition geometries are considered in this study. The surface acquisition geometry is represented by the receivers located along a straight line along the x direction on the upper boundary of the working area, and well acquisition geometry is represented by straight line along the y direction in the working area, which is shown in Figure 2. The asterisk at the center of working area represents the source location. Figures 2a and 2b, respectively, represent the surface acquisition geometry and the acquisition geometry involving both surface and well receivers.

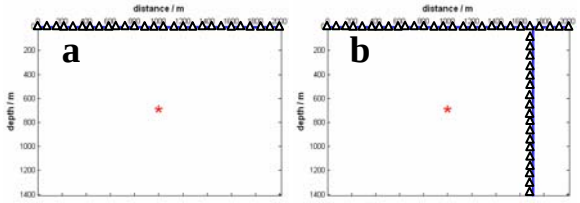

Figure 2: Two types of acquisition geometry used for source imaging. a: receivers on surface; b: receivers on surface and in well.

Figure 3 illustrates the relation between forces and faults for a double-couple source. In reality the radiation patterns of most earthquakes are double-couple. So we focus on the imaging of double-couple sources.

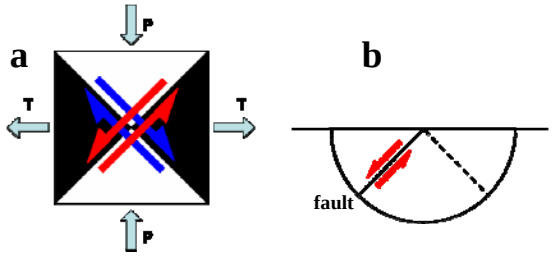

Figure 3: Double-couple source mechanism and corresponding fault type (Stein and Wysession, 2003). a: relation between faults and force direction, P and T represent maximum and minimum compressive stress axis respectively; b: focal sphere side view, which shows the fault type in depth slice.

The true radiation pattern of a double-couple source is calculated by elastic forward modeling (Kosloff *et al*, 1984), and shown in Figure 4. We consider the radiation pattern calculated by forward modeling (Figure 4) as true source radiation pattern, and compare that with the imaged source radiation pattern (Figure 5a and 5d).

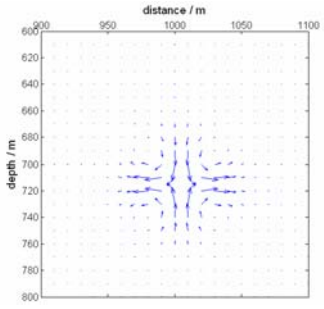

Figure 4: Radiation pattern of a double-couple source (Only the area surrounding source is shown here.)

The amplitude of the imaged source and the true source are compared after normalization, i.e. divide the displacement wave field of the true source and the imaged source by the maximum amplitude of their wave field respectively. The normalized amplitude is compared in Figure 5b and Figure 5e. To estimate the difference between the imaged source and the true source we define relative amplitude (R) as:

$$R = 20\log_{10}\left(\frac{A_I - A_T}{A_T} + 1\right), \qquad (1)$$

where A_I and A_T represent the displacement amplitude of the imaged source and that of the true source. The constant 1 in equation is to avoid the zero values in log calculation and keep the original zero value. The distributions of relative amplitude for receivers on surface and receivers both on surface and in well are shown in Figure 5c and Figure 5f.

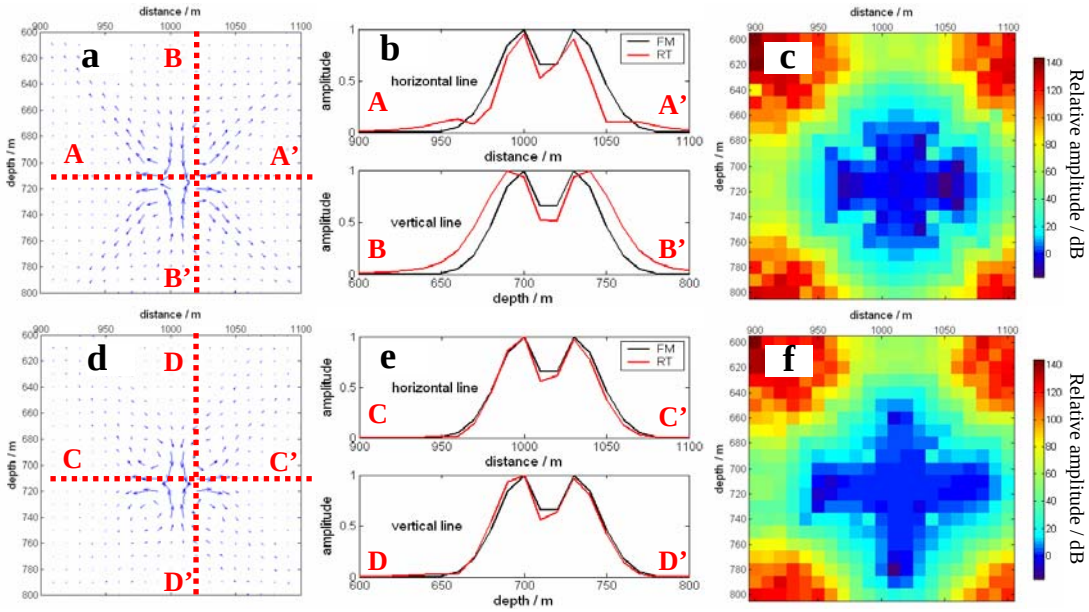

Figure 5: Source radiation patterns and amplitude distributions imaged using surface receivers versus using both surface and well receivers. a, b, and c are images using surface receivers; d, e, and f are images using receivers on surface and in well. a and d are imaged radiation patterns; b and e illustrate the difference between amplitude of true source (black lines, FM) and imaged source (red lines, RT), which represent the absolute amplitude value along the red dotted line in a and d; c and f shows the distribution of relative amplitude defined by equation (1).

In Figure 5c and f the blue color represents the zero value in the relative amplitude, i.e. the best match between the imaged source and the true source. Figure 5f has bigger blue bands with value near-zero in both distance and depth direction than Figure 5c. This is the same with the amplitude comparison in Figure 5b and Figure 5e, which are represented by red dashed perpendicular lines (AA', BB', CC', and DD') in Figure 5a and Figure 5d. The acquisition geometry with receivers in both surface and wellbore has larger aperture than that with only surface receivers. Clearly the acquisition geometry with larger aperture resulted in better source imaging.

The radiation pattern of a source consists of not only amplitude variation but also distribution in the displacement vector.

Figure 6 shows the angle distribution of source radiation pattern. Figure 6a is the angular distribution of the true source. Figure 6b and 6c show the absolute angle distribution of the imaged source's displacement orientation. The angular orientation distribution of the imaged source does not provide much information if we consider the angular distribution in the whole wave field, because the artifacts caused by wave type converting and boundary effect will be significant out of source location area, where the original elastic wave amplitude will be small. We therefore focused on the area surrounding the source area, i.e. the area circled by dashed line in Figure6. Comparing with Figure 6a the angle distribution of the imaged source by the combined geometry is better than that recovered by surface geometry, especially in the area with displacement vector around 45 degree and 0 degree. So the orientation distribution of displacement vector imaged by large aperture is better than that imaged by small aperture. Now we can see that the radiation pattern imaged by large aperture geometry is better than that imaged by small aperture geometry.

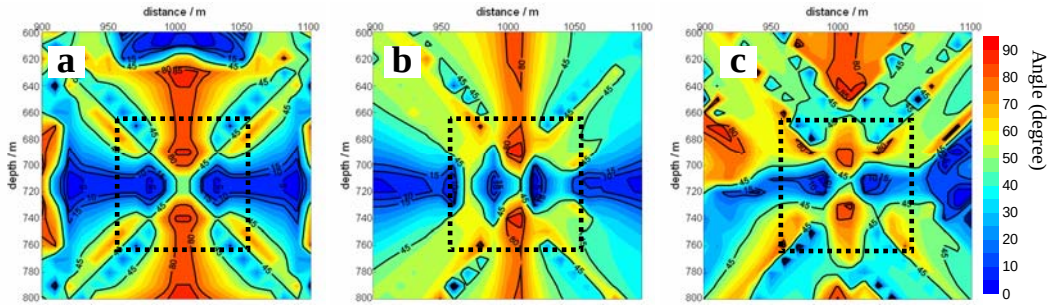

Figure 6: Far-field angular orientation of seismic motions of true source and source imaged by different acquisition geometries a: true source; b: source imaged by surface receivers; c: source imaged by receivers both on surface and in well

Conclusions

Reverse time modeling is an efficient way to recover the source location and radiation pattern. However, it is important to evaluate the factors that influence the quality of mapping the microseismicity. Here we analyze two main factors, the acquisition geometry and data components.

One way to improve the precision of imaging microseismicity is to use multi-component data. Using single component data, no matter whether it is the horizontal or vertical component, can result in a mirror source in imaged wave field. The amplitude of this mirror source is the same as that of the true source. However, we can distinguish the true source from the mirror source using two component data for 2D case. This effect is more significant when only a few of monitoring wells are available and their locations are near each other.

Another way to improve the precision of mapping the source location and radiation pattern is to increase the aperture of the acquisition system. For example, combining the surface receivers with wellbore receivers will increase the aperture. The comparison of radiation patterns recovered using only surface geometry versus combined geometry show that large aperture geometry resulted in better source imaging.

Our results also indicate a potential to resolve the source mechanism using reverse time modeling. The results of this study suggest for a way to better design the acquisition geometry for monitoring induced microseismicity.

Acknowledgements:

This work is funded by National Natural Science Foundation of China (40730317) and China Scholarship Council.

EDITED REFERENCES

Note: This reference list is a copy-edited version of the reference list submitted by the author. Reference lists for the 2009 SEG Technical Program Expanded Abstracts have been copy edited so that references provided with the online metadata for each paper will achieve a high degree of linking to cited sources that appear on the Web.

REFERENCES

Baysal, E., D. Kosloff, and J. Sherwood, 1983, Reverse time migration: Geophysics, **48**, 1514–1524.

Chang, W., and G. McMechan, 1987, Elastic reverse-time migration: Geophysics, **52**, 1365–1375.

Gajewski, D., and E. Tessmer, 2005, Reverse modelling for seismic event characterization: Geophysical Journal International, **163**, 276–284.

Hu, L., and G. McMechan, 1988, Elastic finite-difference modeling and imaging for earthquake sources: Geophysical Journal International, **95**, 303–313.

Kosloff, D., M. Reshef, and D. Loewenthal, 1984, Elastic wave calculations by the Fourier method: Bulletin of the Seismological Society of America, **74**, 875–891.

Loewenthal, D., and I. Mufti, 1983, Reversed time migration in spatial frequency domain: Geophysics, **48**, 627–635.

Lu, R., and N. Toksöz, 2008, Locating microseismic events with time reversed acoustics: A synthetic case study: 78th Annual International Meeting, SEG, Expanded Abstracts, 1342–1346.

Stein, S., and M. Wysession, 2003, An introduction to seismology, earthquakes, and earth structure: Blackwell Publishing.

Sun, R., and G. McMechan, 2001, Scalar reverse-time depth migration of prestack elastic seismic data: Geophysics, **66**, 1519–1527.

White, J. E., 1965, Seismic waves: radiation, transmission, and attenuation: McGraw-Hill.